Magnetism in nanopatterned graphite film

Li Chen,[1,2] Decai Yu,[2] and Feng Liu[2,a)]
[1]Department of Physics, Linyi Normal University, Linyi, Shandong 276005, People's Republic of China
[2]Department of Materials Science and Engineering, University of Utah, Salt Lake City, Utah 84112, USA

Using first-principles calculations, we show that nanopatterned graphite films (NPGFs) can exhibit magnetism in analogy to graphene-based nanostructures (GBNs). In particular, graphite films with patterned nanoscale triangular holes and channels with zigzag edges all have ferromagnetic ground states. The magnetic moments are localized at the edges with a behavior similar to that of GBNs. Our findings suggest that the NPGFs form a unique class of magnetic materials. © *2008 American Institute of Physics*. [DOI: 10.1063/1.3033223]

Magnetic properties of graphene-based nanostructures (GBNs) have attracted a lot of recent interest.[1–12] First-principles and mean-field theory calculations have shown that zero-dimensional graphene nanodots (or nanoflakes),[1–4] one-dimensional nanoribbons,[5–10] and two-dimensional nanoholes[11] that consist of zigzag edges can all exhibit magnetism, making them an interesting new class of nanomagnets. The magnetization in GBNs originates from the localized edge states[5,6] that give rise to a high density of states at the Fermi level rendering a spin-polarization instability.[13,14] The ground-state magnetic ordering within such GBN is found to be consistent with the theorem of itinerant magnetism in a bipartite lattice.[15] Furthermore, a simple geometric rule derived from the underlying hexagonal symmetry has been proposed for designing a rich variety of magnetic nanostructures in graphene.[12]

Despite the promise shown by the theoretical studies in magnetic GBNs, however, the experimental realization of these magnetic GBNs remains a big challenge because synthesis of graphene is at first a difficult task before one further makes them into different forms of nanostructures. Here, using first-principles calculations, we show that many of the zigzag edge-induced magnetic properties in GBNs exist also in nanopatterned graphite films (NPGFs). Because graphite film is readily available, we propose that for certain applications the NPGFs may be used as a better candidate of magnetic nanomaterials than the GBNs to circumvent the difficulties associated with graphene synthesis.

To illustrate our point, we consider two limiting cases of NPGFs: one with only the top atomic layer patterned like a GBN supported on a graphite substrate [Figs. 1(a) and 1(b)] and the other with all the atomic layers in the graphite film patterned throughout like a nanochannel in graphite film [Figs. 1(c) and 1(d)]. As an example, we focus on studying the magnetic properties of triangular nanoholes with zigzag edges. In both cases, we found such nanoholes in graphite film exhibit a FM ground state having a very similar behavior as those in graphene.

For the triangular nanoholes supported on the graphite substrate, we consider two atomic configurations: one is an up-triangle as shown in Fig. 1(a) where each edge atom of the nanohole sits on top of an atom in the second layer and the other one is a down-triangle as shown in Fig. 1(b) where each edge atom sits above the center of the hexagon in the second layer. For triangular nanochannels going through the whole graphite film, to maintain the zigzag edges of nanohole in each layer, the size of nanohole in one layer must be different from that in the other layer (the graphite film has an $ABAB\cdots$ two-layer stacking). Figure 1(c) shows an example of up-triangular channel in which the top layer (A layer) has a nine-atom hole (removing nine atoms) and the bottom B-layer has a four-atom hole. Figure 1(d) shows an example of down-triangular channel in which the top A-layer has a nine-atom hole and the bottom B-layer has a 16-atom hole. Note, however, that the up-triangular nanochannel in Fig. 1(c) and the down-triangular nanochannel in Fig. 1(d) are actually the same channel structure of different sizes if one switches the A layer with the B layer.

Our calculations were performed using the pseudopotential plane-wave method within the spin-polarized generalized gradient approximation as before.[10,11] To model the supported nanoholes, we used supercells consisting of one and two layers of substrate film plus a vacuum layer of 11.13 Å (see Fig. 2); to model the nanochannels, we used supercells consisting of periodic stacking of AB layers as in graphite film (see Fig. 3 below). For both cases, we varied the nanohole size from four- to 16-atom hole in two different sizes of rhombus supercells with a basal plane of $7a\times 7a$ (Fig. 1) and $9a\times 9a$, where a is the graphite lattice constant. We used the theoretically determined lattice constant $a=2.46$ Å and interlayer spacing of 3.35 Å. The largest system contains up to 324 atoms. We used a plane wave cutoff of 22.1 Rd. All the edge atoms are saturated with H and the atomic structure is optimized until forces on all atoms are converged to less than

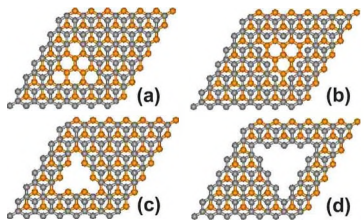

FIG. 1. (Color online) Illustration of atomic structure of supported nanoholes and nanochannels. The C atoms are shown as gray balls in the first layer and orange balls in the second layer. (a) A nine-atom up-triangular nanohole whose edge atoms sit on top of an atom in the second layer. (b) A nine-atom down-triangular nanohole whose edge atoms sit above the center of hexagon in the second layer. (c) An up-triangular nanochannel with a nine-atom nanohole in the first layer and a four-atom nanohole in the second layer. (c) A down-triangular nanochannel with a nine-atom nanohole in the first layer and a 16-atom nanohole in the second layer.

a)Electronic mail: fliu@eng.utah.edu.

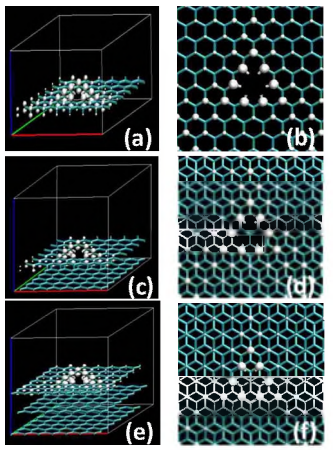

FIG. 2. (Color online) The FM ground-state magnetic configuration of a four-atom triangular nanohole in free and supported graphene. White balls indicate the spin density isosurface at $0.03e/\text{Å}^3$. (a) In a free graphene sheet. (b) Top view of (a). (c) In a graphene sheet supported on one layer of graphite film. (d) Top view of (c). (e) In a graphene sheet supported on two layers of graphite film. (f) Top view of (e).

0.01 eV/Å. For Brillouin zone sampling, we used a $2\times2\times1$ k-point mesh for the case of supported nanoholes and a $2\times2\times4$ mesh for nanochannels, respectively.

The reason we choose the triangular nanoholes is because it is known that such nanoholes have a ferromagnetic (FM) ground state in graphene,[11] as shown in Figs. 2(a) and 2(b). According to the simple geometric designing rule,[12] any two zigzag edges in graphene are FM-coupled if they are at a formal angle of 0° or 120° and antiferromagnetic (AF)-coupled if at an angle of 60° or 180°. Since the three edges in the triangular nanohole are at 120° to each other, they must belong to the same sublattice (A or B) and hence are FM-coupled, consistent with the itinerant magnetism model in a bipartite lattice.[15]

We found that the supported triangular nanoholes have essentially the same behavior, as shown in Figs. 2(c)–2(f). They all have a FM ground-state. For the supported four-atom triangular nanohole in Fig. 2(c), the FM sate is found to be ~17.8 meV lower than the PM state. In fact, the ground-state magnetic configurations of the supported nanoholes are almost identical to those of the corresponding nanoholes in free graphene sheet, as one compares Figs. 2(c) and 2(e) with Fig. 2(a), and Figs. 2(d) and 2(f) with Fig. 2(b). The magnetic moments are largely localized on the edge atoms and decay exponentially moving away from the edge.[11] The calculated total magnetic moment within one unit cell is also found equal to N_B-N_A as predicted from the itinerant magnetism model in bipartite lattice,[15] where N_B (N_A) is the number of atoms on the B-sublattice (A-sublattice) within one unit cell. Consequently, the moment increases with the increasing nanohole size.

The above results indicate that the underlying substrate (graphite film) has a negligible effect on the magnetism of nanoholes in the top "graphene" layer. Physically, this is not too surprising because the magnetism is originated from the localized edge sate from the broken sp^2 type of bonding in the top graphene layer. The edge state is not expected to be affected much by the underlying graphite layer as there exists no strong interlayer "chemical" bonding except weak van de Waals interaction between the top layer and underneath film. For the same reason the magnetic behavior of

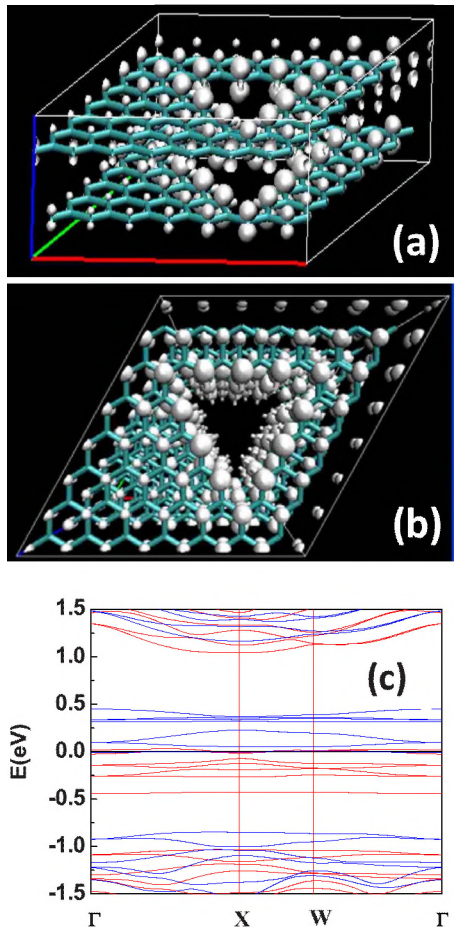

FIG. 3. (Color online) The FM ground-state magnetic configuration of a triangular nanochannel in graphite film consisting of a nine- and 16-atom nanohole in the A and B layer, respectively. (a) The spin density distribution within one supercell. White balls indicate the spin density isosurface at $0.03e/\text{Å}^3$. (b) A perspective view of spin density distribution looking down through the nanochannel. (c) The band structure of the nanochannel of (a).

supported up-triangles are identical with that of down-triangles, although their edge atoms have a different atomic configuration in relation to the layer below [Fig. 1(a) versus Fig. 1(b)].

Also, the above results suggest that despite the electronic structures of graphene are distinctly different from that of graphite film, such as the band structure,[16] the structural defect-originated (or edge-originated) magnetic structure in graphene can be very similar (in the above case almost identical) to that of graphite film. Practically, this finding can be very important with rather useful implications in potential applications of graphite-based nanomagnetic materials. Because graphene and GBNs are very difficult to synthesize, instead we may use NPGFs for creating the similar nanomagnetic structures since graphite film is readily available. For example, graphene nanohole superlattices have been proposed to be used as magnetic storage media;[11] now it is possible to pattern such nanohole superlattices in the top layer of a graphite film without the need of going through the synthetic process of graphene.

In practice, it would be difficult to just pattern the top layer of graphite film. More likely more than one layer of graphite film will be patterned through at the same time. Therefore, it will be interesting as well as useful to know what the magnetic properties of stacked nanoholes in a

graphite film are, or more importantly whether the magnetism will survive in such stacked nanoholes. To answer this question, we have calculated the magnetic properties of nanochannels (infinite number of stacked nanoholes) in a graphite film, as shown in Fig. 3. It represents the other limiting case opposite to the case of one layer of nanohole supported on the graphite film (Fig. 2).

Again, we found that all the triangular nanochannels have a FM ground state, as illustrated by the ground-sate spin-density plots of a nanochannel in Figs. 3(a) and 3(b). For this particular nanochannel, the FM state is calculated to be ~24 meV/unit cell lower than the AF state and ~56.3 meV/unit cell lower than the PM state. The overall magnetic behavior of individual nanoholes in the nanochannel is similar to that of nanoholes in a single graphene layer (either free or supported). The magnetic moments are mostly localized at the edge and decay away from the edge. The total moments increase with the increasing nanochannel size or nanohole size in each layer for the fixed cell size and decrease with the increasing cell size or decreasing nanochannel density for the fixed nanochannel size.

However, quantitatively we found that in a nanochannel the total moments around a nanohole in each layer of graphite film no longer equal to $N_B - N_A$ within the layer. This indicates that there exists some magnetic interaction between the moments in the different layers, although the nature of this interaction is not clear. From the practical point of view, such quantitative variation is not that important as long as the FM ground state is retained in the nanochannel so that desirable magnetic nanostructures, such as nanohole superlattices, can be created by nanopatterning of graphite films even though multiple layers of patterned films are involved.

Figure 3(c) shows the band structure of the nanochannel in Fig. 3(a). One interesting point is that the nanochannel is metallic, which is distinctly different from that of a nanohole in graphene which is a semiconductor.[11] The band gap opening in a graphene nanohole is caused by spin polarization, which makes the on-site energy of the spin-up A-edge state differ from that of the spin-down B-edge state.[8] In a nanochannel, the interlayer interaction broadens the distribution of the on-site energies of A- and B-edges making the spin-up A edge states (bands) overlap with the spin-down B-edge bands, closing up the band gap.

Several experiments have observed magnetism in nanographite-based fiber,[17] all-carbon nanofoam,[18] and proton irradiated graphite.[19,20] It is believed that the magnetism in these nanostructures is originated from the intrinsic properties of carbon materials rather than from the magnetic impurities,[19] although the exact origin is not completely clear. The edge magnetism we discuss here provides one possible origin of all carbon-based nanomagnetism.

In conclusion, we have demonstrated that graphite films can become an all-carbon intrinsic magnetic material when nanopatterned with zigzag edges, using first-principles calculations. The magnetism in NPGFs may be localized within one patterned layer or extended throughout all the patterned layers. It is originated from the highly localized edge states in analogy to that in GBNs. Because graphite film is readily available while mass production of graphene remains difficult, we argue that the NPGFs can be superior for many applications that have been proposed for GBNs.

The work is supported by DOE. First-principles calculations are performed on computers at DOE-NERSC and CHPC of Utah.

[1] J. Fernandez-Rossier and J. J. Palacios, Phys. Rev. Lett. **99**, 177204 (2007).
[2] W. L. Wang, S. Meng, and E. Kairas, Nano Lett. **8**, 241 (2008).
[3] M. Ezawa, Phys. Rev. B **76**, 245415 (2007).
[4] O. Hod, V. Barone, and G. E. Scuseria, Phys. Rev. B **77**, 035411 (2008).
[5] K. Nakada, M. Fujita, G. Dresselhaus, and M. S. Dresselhaus, Phys. Rev. B **54**, 17954 (1996).
[6] M. Fujita, K. Wakabayashi, K. Nakada, and K. Kusakabe, J. Phys. Soc. Jpn. **65**, 1920 (1996).
[7] K. Kusakabe and M. Maruyama, Phys. Rev. B **67**, 092406 (2003).
[8] Y. W. Son, M. L. Cohen, and S. G. Louie, Nature (London) **444**, 347 (2006).
[9] L. Pisani, J. A. Chan, B. Montanari, and N. M. Harrison, Phys. Rev. B **75**, 064418 (2007).
[10] B. Huang, F. Liu, J. Wu, B. L. Gu, and W. Duan, Phys. Rev. B **77**, 153411 (2008).
[11] D. Yu, E. M. Lupton, M. Liu, W. Liu, and F. Liu, Nano Res. **1**, 56 (2008).
[12] D. Yu, E. M. Lupton, H. J. Gao, C. Zhang, and F. Liu, Nano Res. **1**, 497 (2008).
[13] J. C. Slater, Phys. Rev. **49**, 537 (1936).
[14] F. Liu, S. N. Khanna, and P. Jena, Phys. Rev. B **42**, 976 (1990).
[15] E. H. Lieb, Phys. Rev. Lett. **62**, 1201 (1989).
[16] T. Ohta, A. Bostwick, T. Seyller, K. Horn, and E. Rotenberg, Science **313**, 951 (2006).
[17] Y. Shibayama, H. Sato, and T. Enoki, Phys. Rev. Lett. **84**, 1744 (2000).
[18] A. V. Rode, E. G. Gamaly, A. G. Christy, J. G. Fitz Gerald, S. T. Hyde, R. G. Elliman, B. Luther-Davies, A. I. Veinger, J. Androulakis, and J. Giapintzakis, Phys. Rev. B **70**, 054407 (2004).
[19] P. Esquinazi, A. Setzer, R. Hohne, C. Semmelhack, Y. Kopelevich, D. Spemann, T. Butz, B. Kohlstrunk, and M. Losche, Phys. Rev. B **66**, 024429 (2002).
[20] P. Esquinazi, D. Spemann, R. Höhne, A. Setzer, K.-H. Han, and T. Butz, Phys. Rev. Lett. **91**, 227201 (2003).